COLOUR VARIATIONS WITH PHASE OF SELECTED REGIONS OF THE LUNAR SURFACE

JOSEPH SIDKY MIKHAIL
Helwan Observatory, Cairo, Egypt

(Received 18 June, 1970)

Abstract. The four colour photometric observations of 15 regions of the lunar surface are reported in this paper. They all confirm the reddening with increasing phase. Observed regions at wide range of phase show an appreciable colour opposition effect. Reddening factors obtained, are larger near full Moon, and smaller at larger phase angles.

1. Introduction

The colour change of the lunar surface with phase was detected by Gehrels *et al.* (1964) who carried out their observations between phase angles ($-45°$ and $+35°$) and ($-50°$ and $+60°$) with many observations near full-Moon. Peacock (1968) studied colour variation with phase using interference filters of rather narrow pass bands. These observations had been extended from $-70°$ to $+110°$ but a negligible number of observations were made by him within about $\pm 10°$ of full-Moon. His results, however, did not agree with those of Gehrels *et al.* (1964) and additional observations were needed.

2. Photoelectric Colorimetry

The colorimetric measurements of the present work were made by the use of three-beam photo-electric photometer attached to the Cassegrain focus ($f/18$) of the 74″ telescope of the Kottamia Observatory. The programme of this study is arranged in cooperation with the Astronomy Department of Manchester University and Kottamia Observatory in Egypt.

The three-beam photometer used is originally designed by Roberts (1964) and built in the workshop of the Astronomy Department of Manchester University. It has three independent amplifiers as well as three photomultipliers of type E.M.I. 9558B with trialkali photocathodes and giving an extended spectral response into the infra-red. The filters have respectively peak transmissions at 4035 Å, 4765 Å, 5538 Å, 6692 Å and 7922 Å with band-width of 100–200 Å. The photometer measures the intensity of the selected areas on the lunar surface instantaneously in three wavelengths.

The nights selected for observations are mostly good photometric nights, cloudless, free from dust, storms and the visibility is good. Table I gives the dates of observations, and the estimated atmospheric conditions prevailing at these dates.

Sixteen regions shown in Figure 1 are observed and chosen in such a way to represent a variety of grounds on the lunar surface and which are easily identified*.

* The region of Plato is reported by J. S. Mikhail, *Icarus* **8**, 117, 1968.

The Moon **2** (1970) 167–201. *All Rights Reserved*

TABLE I

Nights of observation

Dates of Observations	Estimated Meteorological Conditions
1. 6/7 –10–65	Clouds interrupted the observations
2. 8/9 –10–65	Fair good sky
3. 10/11–12–65	Clouds interrupted the observations
4. 11/12–12–65	Clear sky
5. 12/13–12–65	Clear sky, however clouds have appeared and disappeared twice a night
6. 13/14–12–65	It looks like as if slightly milky sky interrupted by clouds once a night
7. 14/15–12–65	It looks like as if slightly milky sky interrupted by clouds once a night
8. 5/6 – 1–66	Clear sky
9. 7/8 – 1–66	Clear sky with little haze on the horizon
10. 12/13– 1–66	Clear sky
11. 4/5 – 2–66	Clear sky
12. 5/6 – 2–66	Clear sky
13. 8/9 – 2–66	Clear sky
14. 10/11– 2–66	Clear sky
15. 2/3 – 5–66	Clear sky
16. 3/4 – 5–66	Clear sky
17. 4/5 – 5–66	Clear sky
17. 4/5 – 5–66	Clear sky
18. 5/6 – 5–66	Clear sky
19. 6/7 – 5–66	Clear sky
20. 7/8 – 5–66	Clear sky
21. 8/9 – 5–66	Clear sky

Plato and the remaining 15 regions are listed in Table II and most of these regions have a reasonably even surface. The coordinates are determined to the nearest half degree from the position of the points on a USAF Lunar Reference Mosaic and are given in Table II. The observed areas have 5 sec arc in diameter. Plato is selected as standard reference region and is observed many times each night of observation. This region is easily recognized as well as having an even bright distribution which causes no fluctuation during the guiding. Its measurements are used as a judgment of the reliability of the behaviour of the photometer and the night for photometric observations. The results for the centre of Plato have already been published (Mikhail, 1968), while the results of the other regions are given in the present paper.

Some of the observed regions show fluctuations which appears as a noise in the recorded signals. They are caused by guiding on a region whose brightness is uneven. This effect is small as it is usually eliminated in the colour index reductions by making the measurements at the same positions on each recorded chart. This is applied for each set of measurements taken instantaneously using certain filters.

3. Method of Reductions

Scales have been prepared to measure directly the intensities recorded on each chart

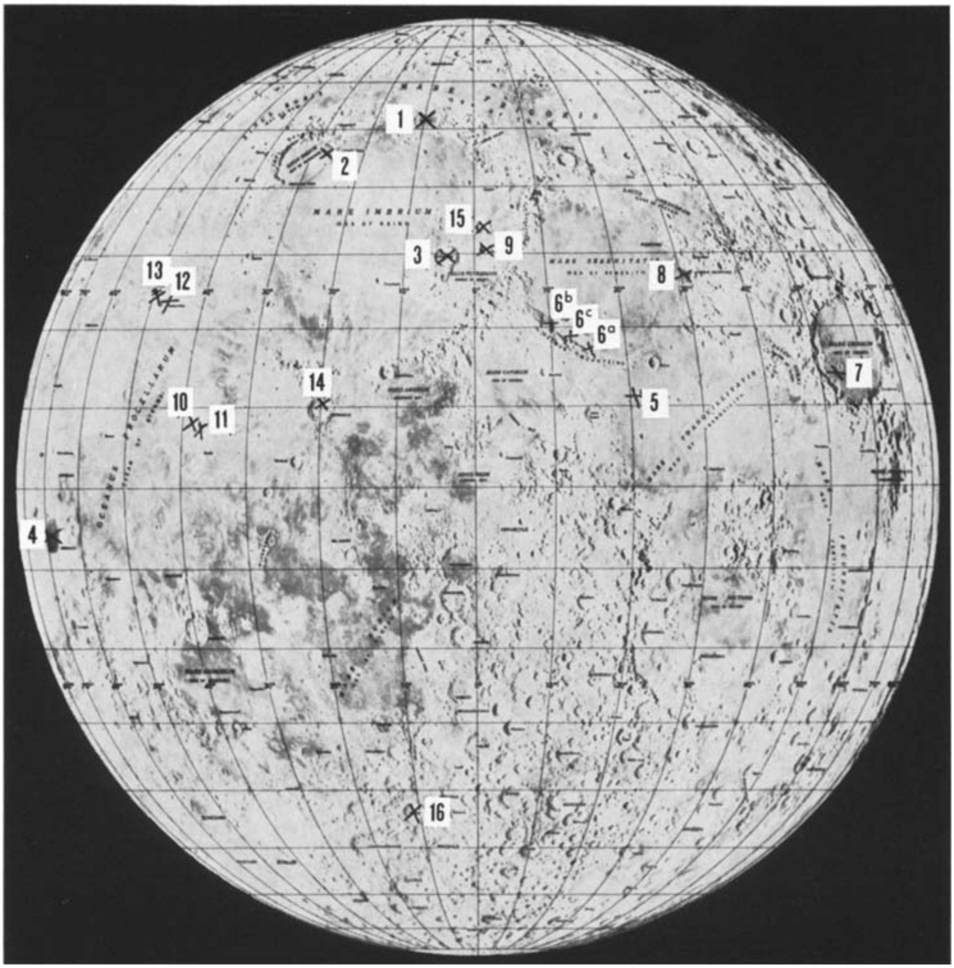

Fig. 1.

in magnitude units. A scale is made for each amplifier taking into account the comparison of the amplifiers and the recorders deflections for different input ranges graduated in steps. Thus, the signals recorded on the charts are read in magnitudes and correspond to that of the amplifiers values. The full scale of the least sensitive step of each amplifier has been selected as standard of a zero magnitude. The other different steps of input ranges are brought to the same scale using the factors of the steps as obtained from the ratios between the load resistors of the steps. The deviation of the real factors from that used to construct the scales is obtained by calibrating the steps. The calibrations are usually a signal record – using a neon lamp – along two consecutive steps and measured in magnitudes by using the scales. The two readings should be equal if the ratio between the two consecutive steps is exactly equal to the

TABLE II

Lunar regions observed at different phases

No. of region		Longitude	Latitude	Name of the region
1		−09° 00′	+52° 30′	PLATO
2		−27 30	+46 00	SINUS IRIDUM
3		−04 00	+29 30	ARCHIMEDES
4		−68 30	−07 00	GRIMALDI
5		+21 00	+11 30	MARE TRANQUILLITATIS
	A	+15 30	+16 30	
6	B	+10 30	+19 30	MARE SERENITATIS
	C	+12 00	+18 30	
7		+54 00	+14 00	MARE CRISIUM
8		+30 30	+27 00	LE MONNIER
9		+02 00	+30 30	AUTOLYCUS
10		−38 30	+08 30	KEPLER
11		−37 30	+07 30	KEPLER RAY SYSTEM
12		−47 30	+23 00	ARISTARCHUS
13		−49 30	+24 00	BRIGHT AREA NORTH-WEST OF ARISTARCHUS
14		−20 30	+10 30	COPERNICUS NORTH
15		+01 30	+34 00	ARISTILLUS
16		−12 00	−44 00	CENTER OF TYCHO

ratio used. As it is not the case in practice, the difference in magnitudes between the two readings is the correction required. These calibrations are repeated for other scales and for every period of observations. Corrections are all referred to the less sensitive step No. 1 which is taken as standard. Table III lists the corrections in magnitudes for each amplifier and step and for each period of observations. Column one gives the amplifiers input steps and the consecutive columns give the correcting factors in magnitudes. It can be seen that there are some variations in the corrections of some periods of observations. These differences are probably due to the big variations in the temperature over a long period through which the program of observations is carried out.

Therefore, the recorded observations are measured in magnitudes using the scales and then corrections for each step are applied using Table III. The measurements are corrected for the background and the dark current.

The atmospheric extinction coefficients are obtained for each night of observations in the usual way by plotting the measured magnitudes of the stars against different values of air masses. The plot shows a straight line from which both the magnitude of the star outside the atmosphere and the atmospheric extinction coefficients can be obtained.

The extinction factors and the stars magnitude at zero atmosphere are deduced for each filter. The extinction factors obtained from the stars measurements are applied to the lunar measurements to account for the effect of the atmosphere. The stellar magnitudes at zero atmosphere are used to provide a zero level for the readings. At

TABLE III

Amplifier no. 1	*Corrections in magnitudes*		
Amplifier input steps	Oct.	Dec., Jan. and Feb.	May
1	0.000^m	0.000^m	0.000^m
2	−0.009	+0.007	+0.005
3	−0.071	−0.051	−0.051
4	−0.080	−0.044	−0.046
5	−0.041	+0.024	+0.014
6	−0.050	+0.031	+0.019
7	−0.103	−0.014	−0.013
8	−0.112	−0.007	−0.008
9	−0.161	−0.070	−0.043

Amplifier no. 2	*Corrections in magnitudes*	
Amplifier input steps	Oct., Dec., Jan., and Feb.	May
1	0.000^m	0.000^m
2	+0.013	−0.016
3	+0.021	−0.036
4	+0.034	−0.052
5	+0.063	−0.042
6	+0.076	−0.058
7	+0.068	−0.092
8	+0.081	−0.108
9	+0.108	−0.110
10	+0.121	−0.126

Amplifier no. 3	*Corrections in magnitudes*	
Amplifier input steps	Oct., Dec., Jan. and Feb.	May
1	0.000^m	0.000^m
2	+0.041	+0.017
3	+0.069	+0.004
4	+0.110	+0.021
5	+0.120	+0.051
6	+0.161	+0.068
7	+0.165	+0.050
8	+0.206	+0.067

each period of observations, the same star is measured on different nights. By reducing the observations to the same value, comparisons are possible from night to night. The relative magnitude measurements of the selected lunar regions measured on different nights of this period are combined.

To combine all the measurements of one colour observed during the period of the eight months of observations, all the stars observed are intercompared. This could be done because two stars are mostly observed during the whole night of observations and used in the reduction of observations to the same level. Table IV lists the observed stars, their positions, spectral type and experimental results of the magnitudes of each star outside the atmosphere reduced to the same level at each wavelength.

The phase angles are computed for the time of observation using the following formula.

$$\cos \alpha = \sin B_0 \sin B_0 + \cos B_0 \cos B_2 \sin (C_2 + \lambda_0)$$

TABLE IV

The observed stars

Star	R.A.	Dec.	Sp. type	m_{4035}	m_{4765}	m_{5538}	m_{6692}	m_{7922}
α Leonis	10.109^h	12.134°	B_8	0.524^m	4.792^m	5.477^m	8.278^m	4.945^m
α Bootis	14.235	19.359	K_0	0.951	4.156	3.984	6.070	2.251
α Canis Minoris	7.625	5.313	F_5	0.242	4.145	4.482	7.000	3.434
ε Orionis	5.575	−1.222	B_0	0.828	5.180	5.858	8.702	5.402
α Arietis	2.088	23.302	K_2	2.963	6.285	6.180	8.340	4.574

where, B_0 and λ_0 are the selenographic latitude and longitude corrected for the topocentric values as explained by Kopal (1962), C_2 is the complement of the Sun's selenographic longitude and B_2 is the Sun's selenographic latitude. The phase angles are positive after full Moon and negative before.

In this way, the lunar feature measurements in magnitudes namely m_{4038}, m_{4765}, m_{5538}, m_{6692} and m_{7922} are deduced where 4035, 4765, 5538, 6692 and 7922 are the wavelengths of the filters used. A series of four colour indices are obtained by subtracting the magnitudes measured instantaneously at different wavelengths. They are within the range of phase angles $-43°$ to $+86°$ including many observations near full Moon. The results of the standard region Plato are published (Mikhail, 1968). The results of the other observed lunar regions are given in Table V where the first and the second columns give the date of observations and the phases respectively while the other consecutive columns contain the observed colour indices.

4. Errors

The 74″ telescope is newly erected and from our experience it is found that its mechanical system is working satisfactorily and during the very short time of observations of individual regions, no guidance errors could be traced. The signals are coherent and the measurements are made for corresponding points on each of the three traces. The read magnitudes of the charts can be measured to an accuracy between $\pm 0.001^m$ to $\pm 0.004^m$ according to the size of the deflection.

From the comparative measurements used as calibrations, the amplifiers are functioning satisfactorily for a period of some days and show small drift in a long period

TABLE V

Date	α	$\frac{5538}{4035}$	$\frac{4765}{7922}$	$\frac{6692}{4765}$	$\frac{6692}{7922}$
*2: SINUS IRIDUM					
11/12–12–65	+45.9	3.547	1.625	2.216	3.840
13/14–12–65	+72.2	3.541	1.633	2.159	3.785
14/15–12–65	+85.6	3.491	1.635	2.160	3.796
5/6 – 1–66	−17.6	3.602	1.585	2.151	3.736
7/8 – 1–66	+10.5	3.618	1.566	2.161	3.741
	+11.4	3.612	1.547	2.191	3.738
12/13– 1–66	+79.9	3.496	1.624	2.228	3.851
4/5 – 2–66	−10.4	3.601	1.628	.....	.....
5/6 – 2–66	+ 5.6	3.625	1.495	2.226	3.720
8/9 – 2–66	+48.1	3.586	1.596	2.152	3.748
10/11– 2–66	+74.6	3.498	1.602	2.222	3.824
3/4 – 5–66	−13.6	3.713	1.486	2.254	3.740
4/5 – 5–66	+ 1.5	3.678	1.398	2.279	3.676
5/6 – 5–66	+13.3	3.600	1.555	2.216	3.771
6/7 – 5–66	+27.7	3.578	1.550	2.220	3.770
7/8 – 5–66	+38.9	3.630	1.577	2.187	3.764
8/9 – 5–66	+51.3	3.547	1.600	2.186	3.786
3: ARCHIMEDES					
6/7 –10–65	−43.6	3.326	1.669	2.075	3.744
11/12–12–65	+44.9	3.565	1.576	2.194	3.770
13/14–12–65	+72.3	3.556	1.614	2.193	3.808
14/15–12–65	+85.6	3.585	1.587	2.206	3.792
5/6 – 1–66	−17.8	3.599	1.560	2.192	3.752
7/8 – 1–66	+10.8	3.644	1.507	2.202	3.709
12/13– 1–66	+79.8	3.530	1.603	2.229	3.831
4/5 – 2–66	−11.8	3.632	1.560	2.181	3.742
5/6 – 2–66	+ 5.8	3.667	1.436	2.268	3.704
	+ 7.9	3.726	1.382	2.330	3.714
8/9 – 2–66	+48.3	3.616	1.530	2.198	3.728
10/11– 2–66	+74.1	3.559	1.578	2.231	3.809
2/3 – 5–66	−27.2	3.676	1.556	2.201	3.757
3/4 – 5–66	−13.7	3.719	1.549	2.185	3.734
4/5 – 5–66	− 0.9	3.646	1.473	2.251	3.724
	+ 1.4	3.705	1.352	2.325	3.677
5/6 – 5–66	+13.5	3.635	1.491	2.269	3.760
6/7 – 5–66	+26.0	3.638	1.510	2.224	3.734
7/8 – 5–66	+39.4	3.646	1.540	2.239	3.779
8/9 – 5–66	+50.9	3.576	1.562	2.207	3.769
4: GRIMALDI					
11/12–12–65	+46.0	3.626	1.546	2.250	3.795
12/13–12–65	+59.5	3.650	1.570	2.244	3.814
14/15–12–65	+86.0	3.582	1.554	.....	.....
7/8 – 1–66	+10.8	3.675	1.482	2.234	3.716
12/13– 1–66	+80.2	3.547	1.589	2.251	3.841
4/5 – 2–66	−10.4	3.652	1.529	2.236	3.766
5/6 – 2–66	+ 5.9	3.684	1.422	2.293	3.714
8/9 – 2–66	+48.6	3.656	1.487	2.234	3.722
3/4 – 5–66	−13.3	3.673	1.450	2.281	3.731

* The first region 'Plato' is published *Icarus* **8**, 117, 1968.

Table V (Continued)

Date	α	5538/4035	4765/7922	6692/4765	6692/7922
4/5 – 5–66	– 0.9	3.684	1.436	2.270	3.702
	+ 1.4	3.732	1.337	2.340	3.678
5/6 – 5–66	+13.6	3.669	1.464	2.293	3.757
6/7 – 5–66	+27.4	3.615	1.545	2.223	3.768
7/8 – 5–66	+39.5	3.641	1.529	2.246	3.776
8/9 – 5–66	+51.2	3.592	1.548	2.232	3.780
5: MARE TRANQUILLITATIS					
12/13–12–65	+57.8	3.631	1.504	2.290	3.793
	+57.8	3.674	1.502	2.300	3.802
	+57.9	.....	1.514	2.298	3.812
	+58.0	3.684	1.485	2.313	3.798
	+58.0	3.679	1.491	2.266	3.757
7/8 – 1–66	+11.3	3.712	1.473	2.237	3.710
10/11– 2–66	+73.9	3.628	.....	2.366	3.779
5/6 – 5–66	+14.6	3.706	1.415	2.337	3.753
	+14.6	3.688	1.450	2.308	3.757
	+14.6	3.714	1.397	2.364	3.762
	+14.6	3.727	1.416	2.337	3.753
6/7 – 5–66	+27.6	3.658	1.492	2.277	3.769
8/9 – 5–66	+50.9	3.664	1.495	2.291	3.786
	+50.9	3.642	1.500	2.288	3.788
6A: MARE SERENITATIS					
2/3 – 5–66	–26.9	3.713	1.550	2.212	3.762
3/4 – 5–66	–13.2	3.734	1.536	2.190	3.732
4/5 – 5–66	+ 1.6	3.758	1.354	2.338	3.692
5/6 – 5–66	+15.0	3.662	1.448	2.301	3.749
6/7 – 5–66	+26.2	3.646	1.474	2.269	3.743
8/9 – 5–66	+51.0	3.608	1.503	2.265	3.768
6B: MARE SERENITATIS					
12/13– 1–66	+80.1	3.540	1.447	.....	.....
4/5 – 2–66	–10.5	3.642	1.589	2.178	3.767
5/6 – 2–66	+ 7.6	3.712	1.372	2.348	3.720
8/9 – 2–66	+48.5	3.618	1.555	2.245	3.800
10/11– 2–66	+73.8	3.546	1.581	2.222	3.803
2/3 – 5–66	–26.8	3.671	1.594	2.197	3.791
3/4 – 5–66	–13.2	3.755	1.548	2.173	3.721
5/6 – 5–66	+15.1	3.639	1.445	2.304	3.749
6/7 – 5–66	+26.2	3.642	1.505	2.250	3.755
8/9 – 5–66	+51.0	3.571	1.570	2.202	3.773
6C: MARE SERENITATIS					
12/13– 1–66	+80.1	3.586	.....	.....	3.763
4/5 – 2–66	–10.5	3.669	1.521	2.235	3.756
5/6 – 2–66	+ 7.6	3.758	1.322	2.386	3.708
8/9 – 2–66	+48.5	3.637	1.477	.....	.....
10/11– 2–66	+73.8	3.634	.....	.....	3.751
2/3 – 5–66	–26.8	3.729	1.606	2.172	3.778
3/4 – 5–66	–13.2	3.769	1.515	2.194	3.709

Table V (Continued)

Date	α	5538/4035	4765/7922	6692/4765	6692/7922
5/6 – 5–66	+15.0	3.682	1.420	2.331	3.750
8/9 – 5–66	+51.0	3.630	1.484	2.270	3.754
7: MARE CRISIUM					
6/7 –10–65	−42.5	.....	.....	.....	3.727
7/8 – 1–66	+11.3	3.654	1.510	2.204	3.714
4/5 – 2–66	−10.2	3.625	1.609	2.180	3.789
5/6 – 2–66	+ 7.6	3.718	1.347	2.371	3.718
3/4 – 5–66	−13.0	3.729	1.516	2.195	3.711
4/5 – 5–66	+ 1.3	3.715	1.366	2.330	3.696
5/6 – 5–66	+15.0	3.643	1.433	2.322	3.755
6/7 – 5–66	+27.6	3.601	1.508	2.273	3.781
7/8 – 5–66	+39.2	.....	.....	.....	3.861
8: LE MONNIER					
11/12–12–65	+45.0	3.593	1.598	2.249	3.847
12/13–12–65	+58.1	3.660	1.561	2.294	3.855
4/5 – 2–66	−10.6	3.646	1.572	2.194	3.766
5/6 – 2–66	+ 7.6	3.694	1.348	2.369	3.717
2/3 – 5–66	−27.0	3.688	1.568	2.201	3.769
3/4 – 5–66	−13.3	3.735	1.560	2.167	3.727
4/5 – 5–66	+ 1.3	3.699	1.387	2.320	3.707
5/6 – 5–66	+14.5	3.658	1.471	2.301	3.771
6/7 – 5–66	+26.2	3.663	1.500	2.257	3.757
7/8 – 5–66	+39.2	3.650	1.533	2.264	3.797
8/9 – 5–66	+51.0	3.612	1.563	2.227	3.790
9: AUTOLYCUS					
6/7 –10–65	−43.6	3.674	1.634	2.103	3.737
11/12–12–65	+45.0	3.560	1.584	2.195	3.779
5/6 – 1–66	−17.8	3.610	1.523	2.228	3.751
4/5 – 2–66	−11.7	3.646	1.534	2.205	3.739
5/6 – 2–66	+ 5.8	3.666	1.447	2.234	3.680
2/3 – 5–66	−27.1	3.669	1.500	2.228	3.728
3/4 – 5–66	−13.7	3.697	1.511	2.196	3.707
5/6 – 5–66	+13.5	3.622	1.478	2.266	3.744
6/7 – 5–66	+26.1	3.643	1.511	2.225	3.737
8/9 – 5–66	+50.9	3.569	1.574	2.196	3.772
10: KEPLER					
11/12–12–65	+45.1	3.597	1.441	2.282	3.722
12/13–12–65	+59.6	3.647	1.534	2.235	3.769
13/14–12–65	+72.9	3.571	1.562	2.210	3.772
14/15–12–65	+85.8	3.557	1.539	2.226	3.765
5/6 – 1–66	−17.7	3.616	1.457	2.262	3.719
7/8 – 1–66	+10.9	3.680	1.468	2.237	3.705
12/13– 1–66	+79.9	3.532	1.613	2.176	3.789
4/5 – 2–66	−11.6	3.688	1.479	2.243	3.722
5/6 – 2–66	+ 5.5	3.689	1.440	2.226	3.666
8/9 – 2–66	+48.2	3.646	1.486	2.206	3.693
2/3 – 5–66	−27.3	3.720	1.455	2.271	3.726

Table V (Continued)

Date	α	$\frac{5538}{4035}$	$\frac{4765}{7922}$	$\frac{6692}{4265}$	$\frac{6692}{7922}$
3/4 - 5–66	−13.5	3.691	1.434	2.256	3.691
4/5 - 5–66	− 0.9	3.674	1.375	2.296	3.670
	+ 1.4	3.722	1.303	2.361	3.664
5/6 - 5–66	+13.6	3.669	1.464	2.293	3.757
6/7 - 5–66	+27.4	3.605	1.454	2.253	3.707
7/8 - 5–66	+39.3	3.644	1.470	2.268	3.739
8/9 - 5–66	+50.8	3.549	1.514	2.211	3.724
11: KEPLER RAY SYSTEM					
11/12–12–65	+45.2	3.561	1.466	2.211	3.678
13/14–12–65	+72.8	3.570	1.572	2.162	3.734
14/15–12–65	+85.9	3.555	1.530	2.194	3.724
5/6 - 1–66	−17.7	3.617	1.477	2.254	3.731
7/8 - 1–66	+10.9	3.666	1.488	2.222	3.710
12/13- 1–66	+80.0	3.553	1.577	2.200	3.777
4/5 - 2–66	−11.6	3.663	1.494	2.223	3.717
5/6 - 2–66	+ 5.5	3.655	1.477	.....	3.673
8/9 - 2–66	+48.2	3.621	1.485	2.211	3.696
2/3 - 5–66	−27.3	3.694	1.528	2.210	3.738
3/4 - 5–66	−13.5	3.683	1.481	2.210	3.692
4/5 - 5–66	− 0.9	3.657	1.409	2.268	3.677
	+ 1.3	3.717	1.316	2.352	3.668
5/6 - 5–66	+13.7	3.623	1.420	2.296	3.717
6/7 - 5–66	+27.4	3.604	1.476	2.239	3.716
7/8 - 5–66	+39.3	3.636	1.496	2.248	3.744
8/9 - 5–66	+50.8	3.568	1.508	2.221	3.729
12: ARISTARCHUS					
12/13–12–65	+59.5	3.694	1.369	2.335	3.703
13/14–12–65	+72.9	3.573	1.543	2.148	3.691
14/15–12–65	+86.0	3.540	1.540	2.211	3.751
7/8 - 1–66	+10.9	3.671	1.461	2.243	3.704
12/13- 1–66	+80.0	3.516	1.559	2.208	3.767
4/5 - 2–66	−11.6	3.698	1.479	2.236	3.716
5/6 - 2–66	+ 5.6	3.673	1.401	2.261	3.662
8/9 - 2–66	+48.1	3.642	1.472	2.214	3.686
3/4 - 5–66	−13.6	3.755	1.514	2.196	3.709
4/5 - 5–66	− 0.7	3.733	1.316	2.350	3.666
4/5 - 5–66	+ 1.2	3.762	1.307	2.356	3.663
5/6 - 5–66	+13.6	3.648	1.404	2.320	3.724
6/7 - 5–66	+27.5	3.684	1.411	2.299	3.710
7/8 - 5–66	+39.0	3.690	1.429	2.282	3.711
8/9 - 5–66	+50.8	3.620	1.470	2.253	3.723
13: BRIGHT AREA NORTH-WEST OF ARISTARCHUS					
12/13–12–65	+59.5	3.653	1.526	2.238	3.764
13/14–12–65	+72.9	3.617	1.406	2.268	3.674
14/15–12–65	+68.0	3.614	1.367	2.314	3.681
7/8 - 1–66	+10.8	3.777	1.306	2.346	3.652
4/5 - 2–66	−11.6	3.760	1.356	2.324	3.680

Table V (Continued)

Date	α	5538/4035	4765/7922	6692/4765	6692/7922
5/6 – 2–66	+ 5.6	3.791	1.244	2.376	3.621
8/9 – 2–66	+48.2	3.478	1.336	2.350	3.636
3/4 – 5–66	−13.5	3.744	1.222	2.408	3.629
4/5 – 5–66	− 0.8	3.686	1.222	2.408	3.630
5/6 – 5–66	+13.6	3.719	1.233	2.427	3.659
4/5 – 5–66	+ 1.4	3.816	1.155	2.464	3.620
6/7 – 5–66	+27.4	3.699	1.267	2.390	3.657
7/8 – 5–66	+40.0	3.741	1.245	2.396	3.640
8/9 – 5–66	+50.8	3.728	1.233	2.397	3.629
14: COPERNICUS NORTH					
11/12–12–65	+45.2	3.584	1.505	2.260	3.765
12/13–12–65	+59.0	3.563	1.523	.....	.....
13/14–12–65	+72.9	3.586	1.562	2.185	3.747
14/15–12–65	+85.7	3.546	1.571	2.210	3.781
5/6 – 1–66	−17.8	3.628	1.522	2.223	3.745
7/8 – 1–66	+10.6	3.647	1.539	2.201	3.740
12/13– 1–66	+79.9	3.569	1.600	2.188	3.787
4/5 – 2–66	−11.7	3.636	1.549	2.198	3.747
5/6 – 2–66	+ 5.6	3.640	1.510	2.182	3.692
8/9 – 2–66	+48.3	3.607	1.536	2.177	3.713
10/11– 2–66	+74.5	3.552	1.571	2.220	3.791
3/4 – 5–66	−13.1	3.665	1.492	2.218	3.710
4/5 – 5–66	+ 1.4	3.688	1.350	2.337	3.687
6/7 – 5–66	+27.7	3.584	1.529	2.205	3.734
8/9 – 5–66	+50.9	3.558	1.553	2.200	3.754
15: ARISTILLUS					
6/7 –10–65	−43.6	3.689	1.627	2.104	3.730
11/12–12–65	+45.0	3.588	1.530	2.231	3.761
5/6 – 1–66	−17.8	3.626	1.476	2.247	3.722
4/5 – 2–66	−11.7	3.661	1.507	2.224	3.731
5/6 – 2–66	+ 5.8	3.673	1.428	2.235	3.663
2/3 – 5–66	−27.1	3.666	1.474	2.249	3.723
3/4 – 5–66	−13.7	3.689	1.500	2.205	3.705
5/6 – 5–66	+13.6	3.613	1.471	2.260	3.731
6/7 – 5–66	+26.1	3.642	1.443	2.253	3.696
8/9 – 5–66	+50.9	3.561	1.544	2.215	3.759
16: CENTER OF TYCHO					
11/12–12–65	+45.9	3.629	1.431	2.325	3.756
4/5 – 2–66	−10.3	3.650	1.530	2.227	3.757
5/6 – 2–66	+ 7.4	3.771	1.308	2.351	3.659
8/9 – 2–66	+48.6	3.599	1.557	2.216	3.774
3/4 – 5–66	−13.0	3.668	1.359	2.292	3.651
4/5 – 5–66	+ 1.5	3.737	1.272	2.389	3.660
5/6 – 5–66	+14.9	3.647	1.363	2.334	3.697
6/7 – 5–66	+27.3	3.613	1.424	2.275	3.699
7/8 – 5–66	+39.6	3.655	1.454	2.280	3.734
8/9 – 5–66	+51.2	3.598	1.458	2.266	3.724

of time. This effect is combined with the accuracy of the recorder. The linearity test of the recorder with the amplifier does not indicate any deviation.

Small errors in the extinction values arise from the change in the transparency of the atmosphere along the night. It produces a probable error in the extinction of about ± 0.005 m. The error in the air mass is negligible as it depends mainly on the time of each recording and the time is read to the nearest half minutes of time. This may produce an error of about ± 0.005 in the computed air masses.

The separation between the Moon and the stars may introduce some errors on the results of the extinction applied on the lunar regions at some nights of observations. The estimated error which arises from such separation is of the order of 2% obtained from observing two separate stars in one night. The separations between the Moon and the stars, however, are not much effective, as in most of the nights the measurements in the three colours are instantaneously recorded. The most effective error may arise when observing the Moon at larger air masses. Any error in the deduced values of the extinction will be multiplied by the large value of air masses.

The standard error of the deduced colour indices of each night of observations, obtained from repeating the observations of the standard region many times per night are mostly less than 0.01 magnitude. The m_{6692} of the comparison stars used in the reductions has been affected by the level of signal-to-noise. The m_{4038} is the most likely to be influenced by atmospheric extinction. Due to the fact that observation are made over a period of eight months besides the previous reasons, the combined results have an estimated error not greater than ± 0.02 magnitude.

5. Discussions of the Results

The change of the colour indices of the fifteen observed lunar regions with phase are given in Table V and are represented in Figures 2–31. The ordinates in each figure is the colour index on an arbitrary scale and the abscissa is the phase angles. In these

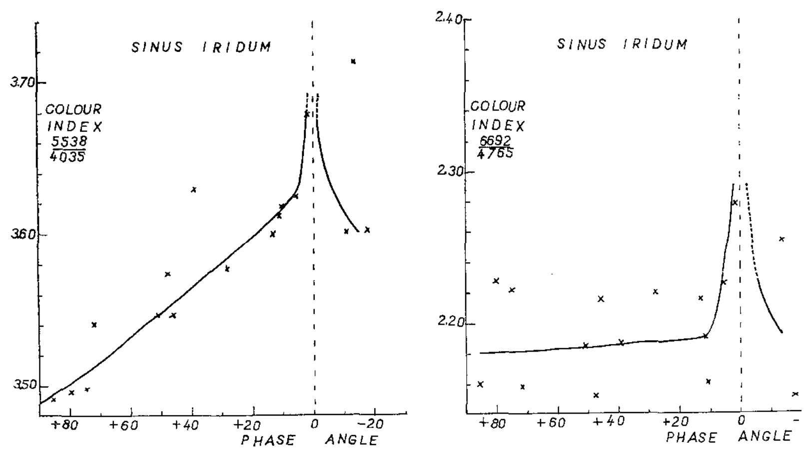

Fig. 2

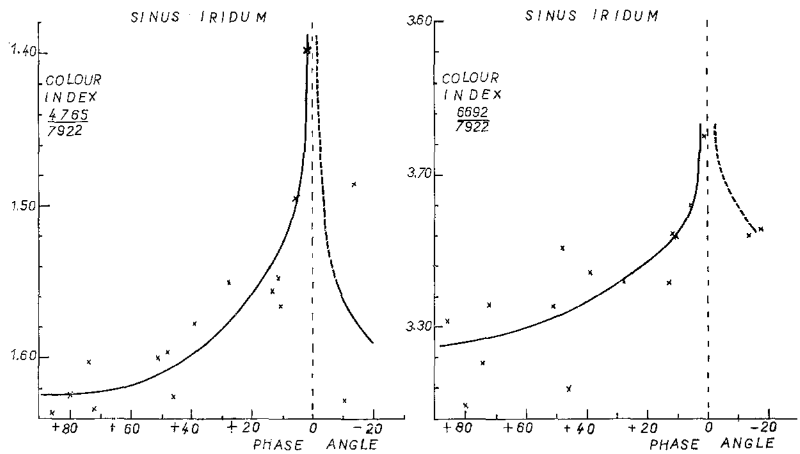

Fig. 3.

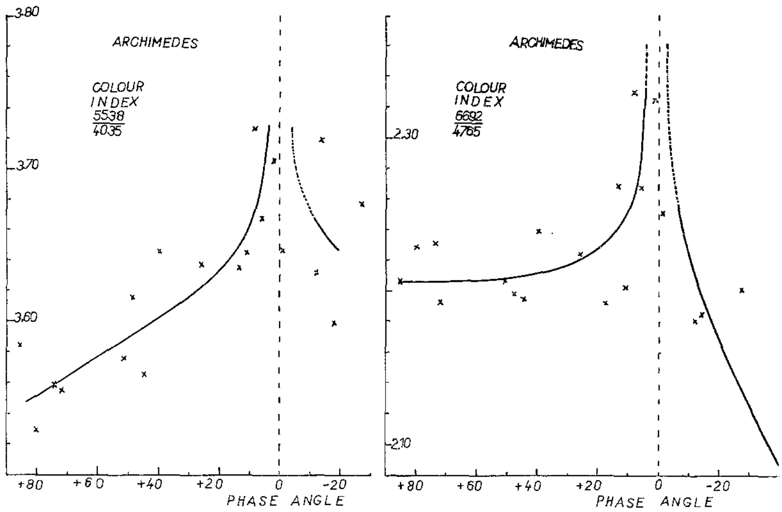

Fig. 4.

figures the best plots are fitted and from which it can be seen that the scatter of the points is reasonable. The colour changes in each figure show three different parts. The first part represents the change in colour between phase angles 10° and 86° after full-Moon, the second part is for phase angles between $\pm 10°$ and 0° and the third part is for phase angle range $-10°$ to $-44°$ before full-Moon.

The variation in the colour index in all figures gives indication that the Moon is bluest at the time of its full and is growing redder towards both quarters. The most fundamental property is the colour-opposition effect of the lunar surface which is an appreciable change in the colour index of the lunar regions near full-Moon. With few exceptions, the effect appears in all the observed regions using different wavelengths.

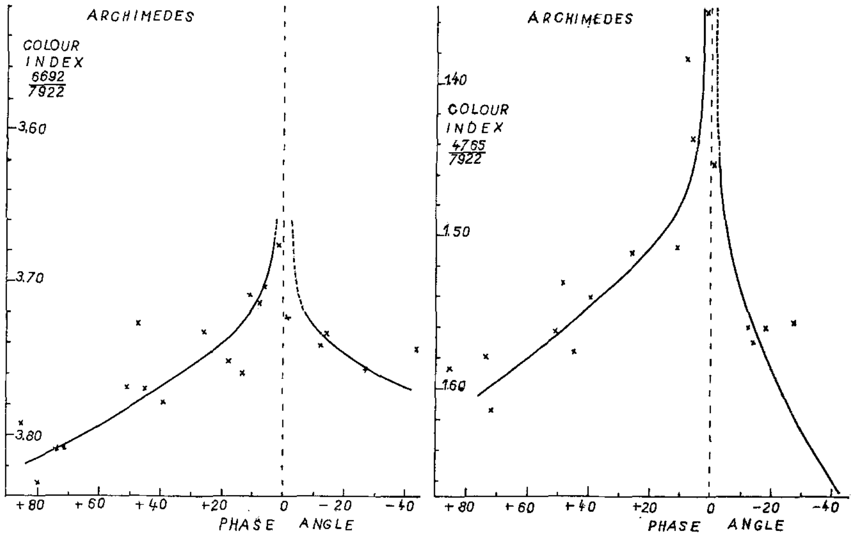

Fig. 5.

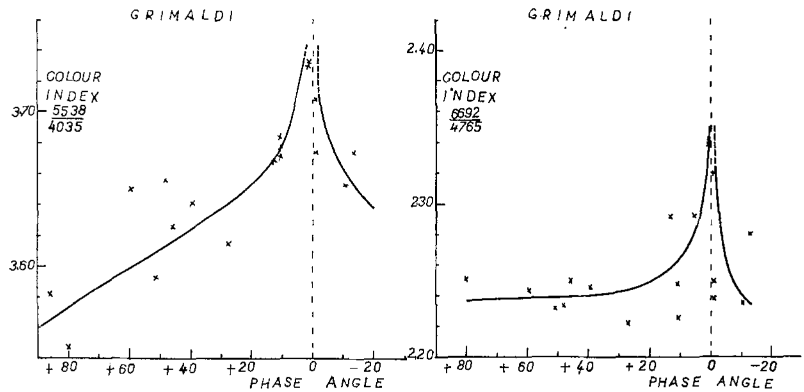

Fig. 6.

Tables VI and VII list the phase factors of reddening after and before full-Moon respectively, where the phase factors of reddening is the rate of increase of the colour index per one degree of phase angle. In each table, the first column records the observed lunar regions while the four consecutive columns give the reddening factors and the standard errors of observations and the limiting range of phase angles for the colour indices $\frac{4035}{5538}$, $\frac{4765}{6692}$, $\frac{4265}{7922}$ and $\frac{6692}{7922}$. The order of reddening in magnitudes near opposition which is the sudden change in the colour index expressed in magnitudes in about 10° due to opposition effect, are listed in Table VIII. The first column records the observed lunar regions and the four consecutive columns give the order of reddening in magnitudes due to the opposition effect and the limiting range of phase for the colour indices $\frac{4035}{5538}$, $\frac{4765}{6692}$, $\frac{4765}{7922}$ and $\frac{6692}{7922}$.

TABLE VI

Phase factors of reddening after full moon

Region	$\Delta\frac{4035}{5538}/\Delta\alpha$	$\Delta\frac{4765}{6692}/\Delta\alpha$	$\Delta\frac{4765}{7922}/\Delta\alpha$	$\Delta\frac{6692}{7922}/\Delta\alpha$
CENTER OF PLATO	0.0017 ± 0.0003 $10° < \alpha < 86°$	Very little reddening $20° < \alpha < 86°$	0.0015 ± 0.0002 $10° < \alpha < 86°$	0.0012 ± 0.0002 $10° < \alpha < 86°$
SINUS IRIDUM	0.0014 ± 0.0002 $5° < \alpha < 86°$	Very little reddening $10° < \alpha < 86°$	0.0030 ± 0.0010 $5° < \alpha < 40°$ 0.0001 ± 0.0004 $40° < \alpha < 86°$ 0.0014 ± 0.0002 $5° < \alpha < 86°$	0.0018 ± 0.0007 $5° < \alpha < 40°$ 0.0014 ± 0.0009 $40° < \alpha < 86°$ 0.0011 ± 0.0003 $5° < \alpha < 86°$
ARCHIMEDES	0.0015 ± 0.0003 $10° < \alpha < 86°$	Very little reddening $20° < \alpha < 86°$	0.0018 ± 0.0002 $10° < \alpha < 86°$	0.0013 ± 0.0003 $10° < \alpha < 86°$
GRIMALDI	0.0015 ± 0.0003 $10° < \alpha < 86°$	Very little reddening $10° < \alpha < 86°$	0.0023 ± 0.0008 $10° < \alpha < 40°$ 0.0008 ± 0.0006 $40° < \alpha < 86°$ 0.0013 ± 0.0003 $10° < \alpha < 86°$	0.0014 ± 0.0004 $10° < \alpha < 86°$
MARE TRANQUILLITATIS	0.0014 ± 0.0002 $15° < \alpha < 80°$	Very little reddening $15° < \alpha < 60°$	0.0008 ± 0.0003 $15° < \alpha < 70°$	0.0007 ± 0.0002 $15° < \alpha < 80°$
MARE SERENITATIS A	0.0015 ± 0.0002 $15° < \alpha < 50°$	0.0007 ± 0.0006 $20° < \alpha < 50°$	0.0015 ± 0.0004 $15° < \alpha < 50°$	0.0016 $0 < \alpha < 50°$
B	0.0020 ± 0.0002 $15° < \alpha < 80°$	0.0009 ± 0.0006 $20° < \alpha < 80°$	0.0017 ± 0.0006 $20° < \alpha < 80°$	0.0010 ± 0.0002 $5° < \alpha < 80°$
C	0.0011 ± 0.0003 $15° < \alpha < 80°$	0.0017 $20° < \alpha < 50°$	0.0018 ± 0.0002 $15° < \alpha < 50°$	0.0007 ± 0.0003 $5° < \alpha < 80°$
MARE CRISIUM	0.0022 ± 0.0022 $10° < \alpha < 30°$	0.0077 ± 0.0043 $2° < \alpha < 20°$	0.0068 ± 0.0035 $2° < \alpha < 30°$	0.0044 ± 0.0007 $2° < \alpha < 40°$
LE MONNIER	0.0014 ± 0.0010 $10° < \alpha < 60°$	0.0012 ± 0.0008 $10° < \alpha < 60°$	0.0028 ± 0.0007 $10° < \alpha < 60°$	0.0019 ± 0.0008 $10° < \alpha < 60°$
AUTOLYCUS	0.0025 ± 0.0005 $5° < \alpha < 50°$	0.0017 ± 0.0006 $5° < \alpha < 50°$	0.0031 ± 0.0003 $5° < \alpha < 50°$	0.0022 ± 0.0004 $5° < \alpha < 50°$
KEPLER	0.0019 ± 0.0004 $10° < \alpha < 86°$	0.0009 ± 0.0004 $10° < \alpha < 86°$	0.0018 ± 0.0003 $5° < \alpha < 86°$	0.0012 ± 0.0006 $5° < \alpha < 86°$

Table VI (Continued)

Region	$\Delta \frac{4035}{5538}/\Delta\alpha$	$\Delta \frac{4765}{6692}/\Delta\alpha$	$\Delta \frac{4765}{7922}/\Delta\alpha$	$\Delta \frac{6692}{7922}/\Delta\alpha$
KEPLER RAY SYSTEM	0.0017 ± 0.0003	0.0011 ± 0.0003	0.0013 ± 0.0003	0.0007 ± 0.0003
	$10° < \alpha < 86°$	$10° < \alpha < 86°$	$5° < \alpha < 86°$	$10° < \alpha < 86°$
ARISTARCHUS	0.0012 ± 0.0004	0.0018 ± 0.0007	0.0016 ± 0.0004	0.0004 ± 0.0003
	$10° < \alpha < 86°$	$5° < \alpha < 86°$	$10° < \alpha < 86°$	$10° < \alpha < 86°$
BRIGHT AREA IN	0.0015 ± 0.0006	0.0014 ± 0.0006	0.0018 ± 0.0006	0.0006 ± 0.0004
ARISTARCHUS REGION	$10° < \alpha < 86°$	$10° < \alpha < 86°$	$5° < \alpha < 86°$	$10° < \alpha < 86°$
COPERNICUS NORTH	0.0013 ± 0.0002	Very little reddening	0.0006 ± 0.0003	0.0007 ± 0.0002
	$10° < \alpha < 86°$	$10° < \alpha < 86°$	$10° < \alpha < 86°$	$10° < \alpha < 86°$
ARISTILLUS	0.0024 ± 0.0007	0.0012 ± 0.0006	0.0027 ± 0.0006	0.0025 ± 0.0008
	$5° < \alpha < 50°$	$10° < \alpha < 50°$	$5° < \alpha < 50°$	$5° < \alpha < 50°$
CENTER OF TYCHO	0.0014 ± 0.0008	0.0034 ± 0.0009	0.0046 ± 0.0007	0.0022 ± 0.0003
	$15° < \alpha < 50°$	$2° < \alpha < 50°$	$2° < \alpha < 50°$	$2° < \alpha < 50°$
		0.0061 ± 0.0017	0.0062 ± 0.0022	
		$2° < \alpha < 20°$	$2° < \alpha < 20°$	
		0.0019 ± 0.0016	0.0036 ± 0.0026	
		$20° < \alpha < 50°$	$20° < \alpha < 50°$	

TABLE VII

Phase factors of reddening before full moon

Region	$\Delta \frac{4035}{5538}/\Delta\alpha$	$\Delta \frac{4765}{6692}/\Delta\alpha$	$\Delta \frac{4765}{7922}/\Delta\alpha$	$\Delta \frac{6692}{7922}/\Delta\alpha$
CENTER OF PLATO	0.0020 ± 0.0059 $-10° > \alpha > -30°$	0.0026 ± 0.0022 $-10° > \alpha > -30°$	0.0039 ± 0.0028 $-10° > \alpha > -43°$	0.0024 ± 0.0017 $-10° > \alpha > -30°$
ARCHIMEDES	0.0028 ± 0.0060 $-10° > \alpha > -30°$	0.0046 ± 0.0020 $-10° > \alpha > -43°$	0.0042 ± 0.0008 $-10° > \alpha > -43°$	0.0013 ± 0.0009 $-10° > \alpha > -43°$
AUTOLYCUS	0.0021 ± 0.0020 $-10° > \alpha > -43°$	0.0040 ± 0.0015 $-10° > \alpha > -43°$	0.0043 ± 0.0017 $-10° > \alpha > -43°$	0.0020 ± 0.0021 $-10° > \alpha > -43°$
KEPLER	0.0030 ± 0.0048 $-10° > \alpha > -30°$	0.0017 ± 0.0023 $-10° > \alpha > -30°$	0.0026 ± 0.0089 $-10° > \alpha > -30°$	0.0015 ± 0.0011 $-10° > \alpha > -30°$
KEPLER RAY SYSTEM	0.0020 ± 0.0016 $-10° > \alpha > -30°$	0.0021 ± 0.0022 $-10° > \alpha > -30°$	0.0025 ± 0.0018 $-10° > \alpha > -30°$	0.0015 ± 0.0016 $-10° > \alpha > -30°$
COPERNICUS NORTH	0.0052 ± 0.0061 $-10° > \alpha > -20°$	0.0024 ± 0.0059 $-10° > \alpha > -20°$	0.0034 ± 0.0098 $-10° > \alpha > -20°$	0.0024 ± 0.0063 $-10° > \alpha > -20°$
ARISTILLUS	0.0021 ± 0.0019 $-10° > \alpha > -43°$	0.0026 ± 0.0017 $-10° > \alpha > -43°$	0.0037 ± 0.0015 $-10° > \alpha > -43°$	0.0013 ± 0.0006 $-10° > \alpha > -43°$

TABLE VIII

Order of reddening in magnitudes near opposition for different colour indices

Region	$\frac{4035}{5538}$ In Range of		$\frac{4765}{6692}$ In Range of		$\frac{4765}{7922}$ In Range of		$\frac{6692}{7922}$ In Range of	
CENTER OF PLATO	0.10^m	10°	0.12^m	20°	0.13^m	10°	0.06^m	10°
SINUS IRIDUM	0.07^m	5°	0.10^m	10°	0.11^m	5°	0.05^m	5°
ARCHIMEDES	0.08^m	10°	0.10^m	15°	0.14^m	10°	0.06^m	10°
GRIMALDI	0.06^m	10°	0.09^m	10°	0.15^m	10°	0.07^m	10°
MARE TRANQUILLITATIS	0.07^m	15°	0.08^m	15°	0.15^m	15°	0.08^m	15°
MARE SERENITATIS A	0.10^m	15°	0.06^m	20°	0.11^m	15°	....	..
B	0.06^m	15°	0.08^m	20°	0.12^m	20°	....	..
C	0.09^m	15°	0.08^m	20°	0.11^m	15°	....	..
MARE CRISIUM	0.08^m	10°	....	..	....	..	....	..
LE MONNIER	0.03^m	10°	0.07^m	10°	0.11^m	10°	0.04^m	10°
KEPLER	0.06^m	10°	0.11^m	10°	0.15^m	5°	0.03^m	5°
KEPLER RAY SYSTEM	0.07^m	10°	0.11^m	10°	0.14^m	5°	0.04^m	10°
ARISTARCHUS	0.09^m	10°	0.05^m	10°	0.13^m	10°	0.05^m	10°
BRIGHT AREA IN ARISTARCHUS REGION	0.07^m	10°	0.10^m	10°	0.11^m	5°	0.04^m	10°
COPERNICUS NORTH	0.06^m	10°	0.14^m	10°	0.18^m	10°	0.05^m	10°
CENTER OF TYCHO	0.12^m	10°	0.09^m	20°	....	..	....	..

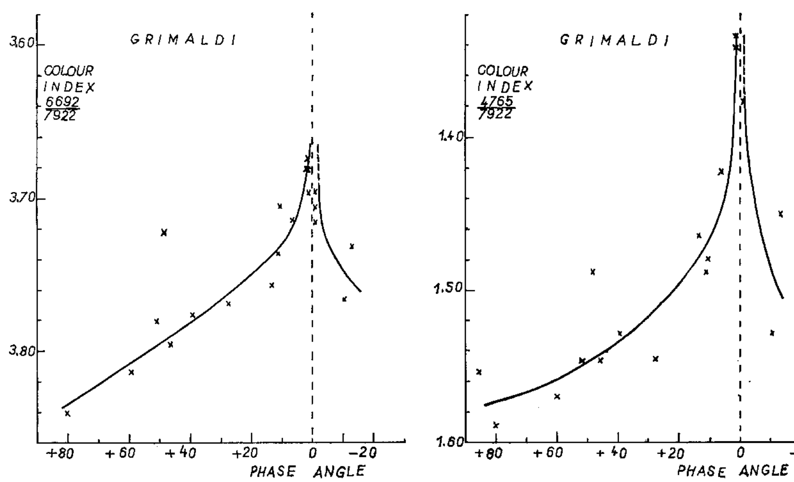

Fig. 7.

The properties of each colour index variation with phase as well as the colour-opposition-effect are discussed separately.

A. THE COLOUR INDEX $(\frac{4035}{5538})$-PHASE VARIATIONS

The colour index variation with phase for the shortest wavelengths 4035 and 5538 Å are given in Figures 2, 4, 6, ... As it is shown in Table VI, the phase factors of reddening are 0.0017^m per degree for the centre of Plato, 0.0014^m for Sinus Iridum,

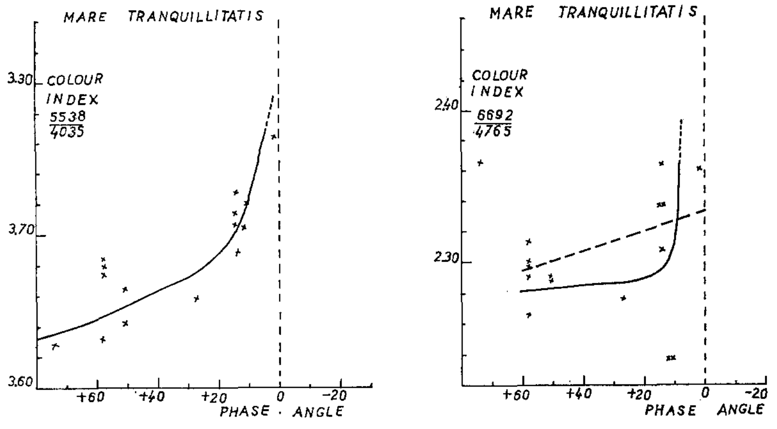

Fig. 8.

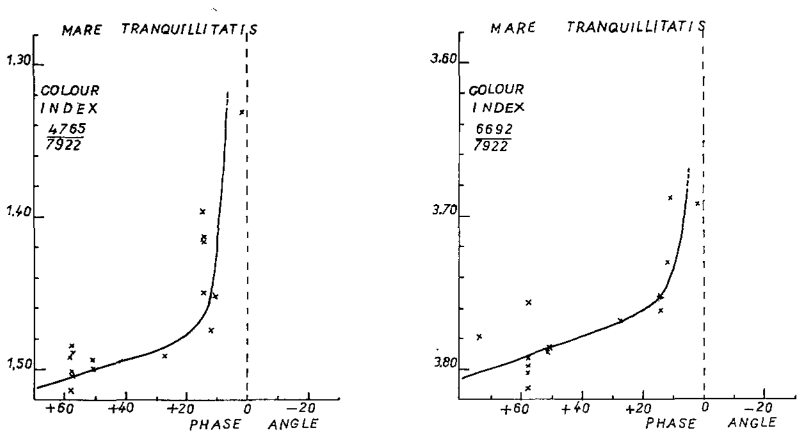

Fig. 9.

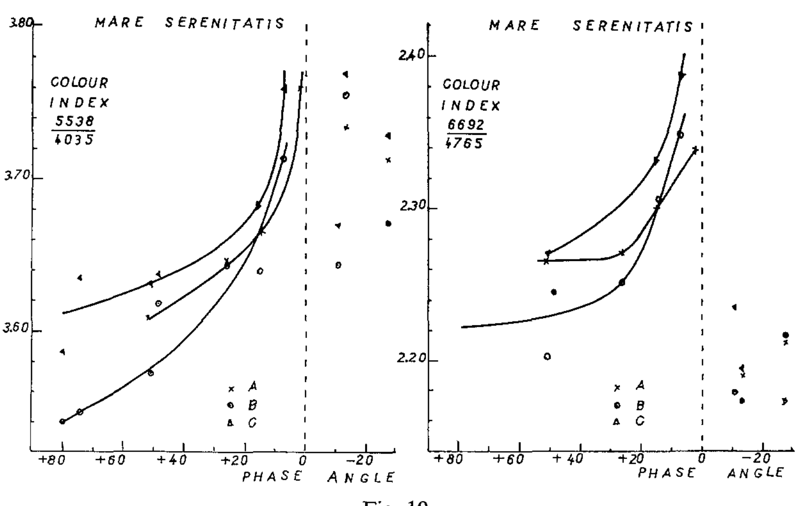

Fig. 10.

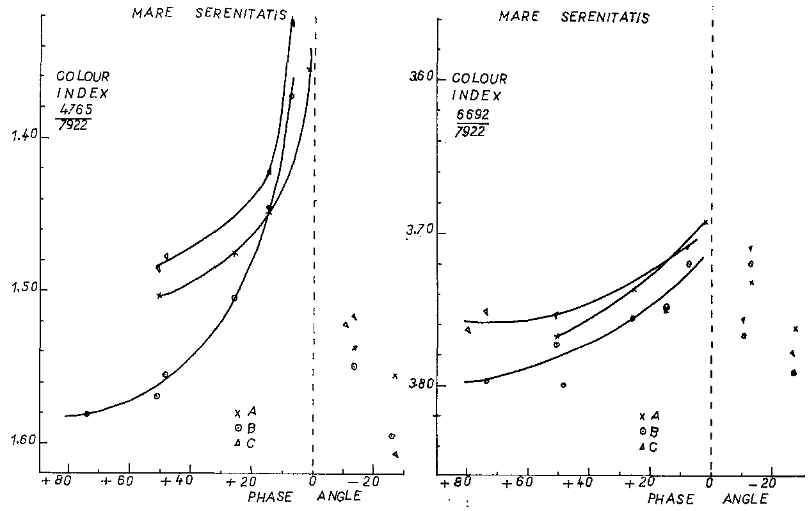

Fig. 11.

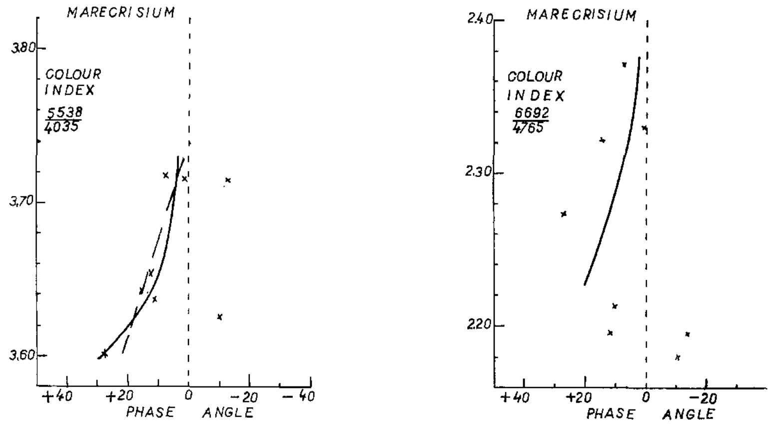

Fig. 12.

0.0015^m for Archimedes, 0.0015^m for Grimaldi, 0.0014^m for Mare Tranquillitatis, 0.0015^m, 0.0020^m and 0.0011^m for the three regions in Mare Serenitatis, 0.0019^m for Kepler, 0.0017^m for Kepler ray system, 0.0012^m for Aristarchus, 0.0015^m for the bright area in the region of Aristarchus and 0.0013^m for Copernicus' north area. All the reddening factors of the previous regions are deduced for phase angles between $\alpha = +10°$ and $+86°$. Within the limits of the errors and over the same range of the phase angles the values of the reddening factors vary slightly for different regions. These regions have different types of grounds and if we assume that they represent generally the features of the lunar surface, then the mean reddening factors of the lunar surface $\lambda = 5538$ Å and $\lambda = 4035$ Å are 0.0015 magnitude per degree.

The areas of Aristillus, Autolycus, Mare Crisium, Le Monnier and Tycho are observed during a limited range of phase angles. Aristillus and Autolycus show relatively high phase factors of reddening of 0.0024^m per degree for Aristillus and 0.0025^m for Autolycus over a range of 50° phase angles. The factor of reddening for Mare Crisium is 0.0022^m per degree for phase angles between $\alpha = 10°$ and 30°. However, the area of Le Monnier shows a factor of 0.0014^m per degree between $\alpha = 10°$ and 60° while the centre of Tycho gives the same factor for a range of observations between $\alpha = 10°$ and 60°.

Generally, before full-Moon, the phase factors of reddening given in Table VII have higher values ranging from 0.0020 to 0.0052 magnitude per degree. The observations are limited in number and ranges of the phase angles which do not exceed 44°. We are not expected to get phase factors of reddening of good accuracy, nevertheless, it indicates reddening with phase.

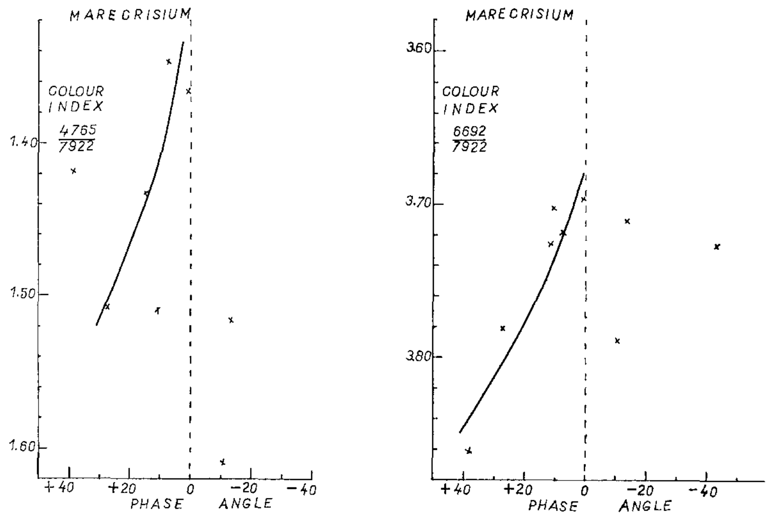

Fig. 13.

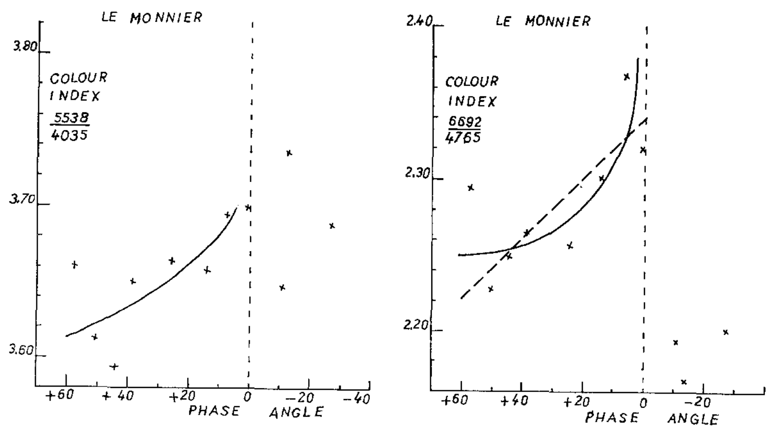

Fig. 14.

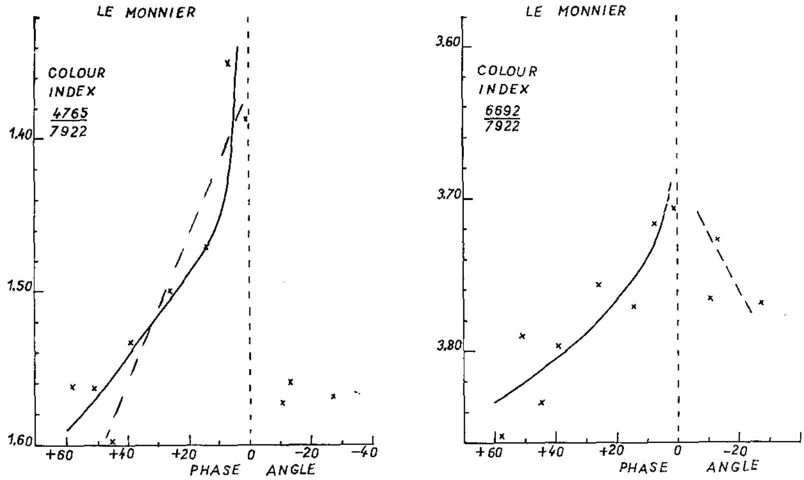

Fig. 15.

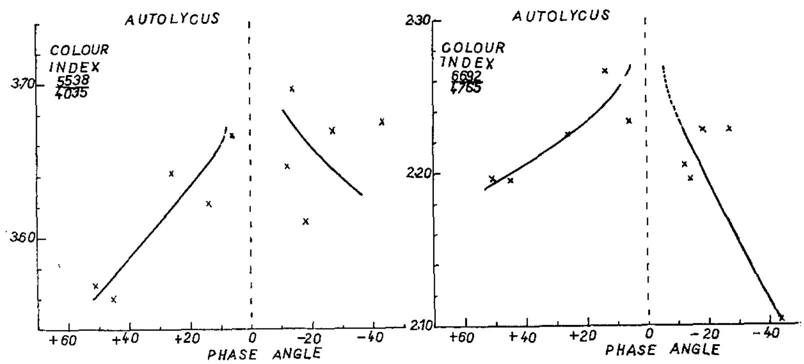

Fig. 16.

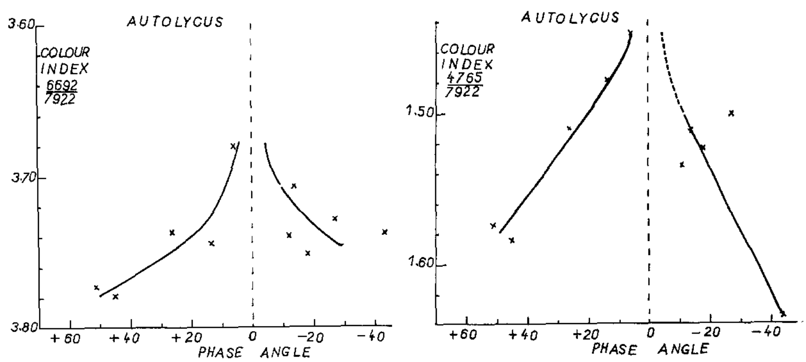

Fig. 17.

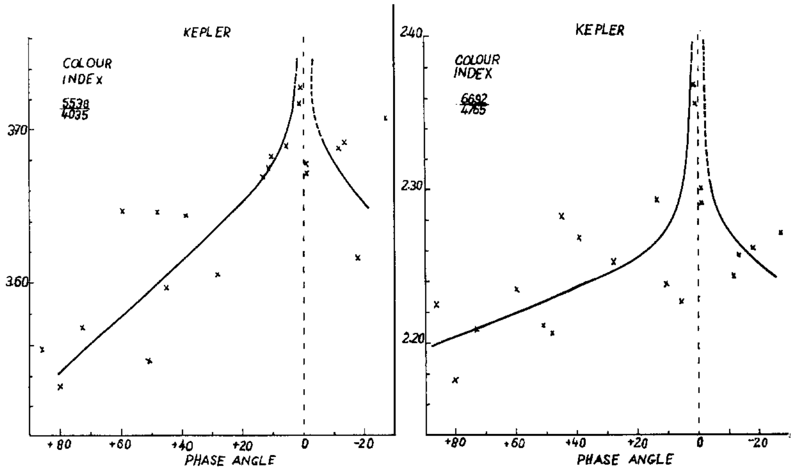

Fig. 18.

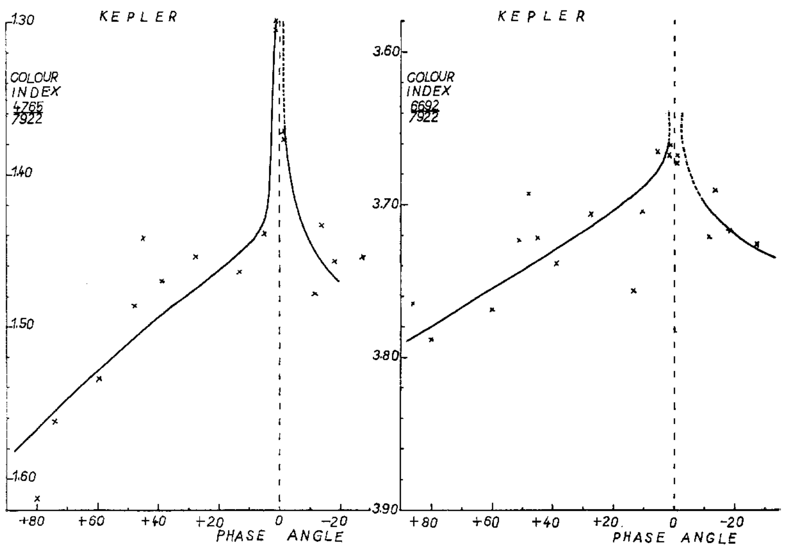

Fig. 19.

B. THE COLOUR INDEX ($\frac{4765}{6692}$)-PHASE VARIATIONS

The change of the colour index with phase after full-Moon between $\alpha = 10°$ and $86°$ for the wavelengths 4765 and 6692 are shown in Figures 2, 4, 6 and 30. As it is given in Table VI, one can divide these values into two groups. The first group is for Plato, Sinus Iridum, Archimedes, Grimaldi, Mare Tranquillitatis and Mare Serenitatis. These regions, except Mare Serenitatis, show slight reddening with phase. The second group is for Kepler, Kepler Ray System, Copernicus north, Aristarchus and the bright area in Aristarchus region. This group except Copernicus north show reddening factors which vary from 0.0009^m per degree for Kepler to 0.0018^m per degree for Aristarchus with a mean value of 0.0013^m per degree. It is worthy to note that the first group is of photovisual albedo of less than 10% while the second group is of photovisual albedo larger than 10% (Kopal, 1966). The regions which show slight reddening after full Moon between $\alpha = 10°$ and 86° show, however, appreciable reddening at small phases. They also tend to show appreciable reddening before full Moon. Observations are required for many other regions on the lunar surface.

As mentioned before, some regions are observed at a limited range of phase angles. These regions show reddening factors of 0.0012^m per degree for Aristillus, 0.0017^m for Autolycus, 0.0012^m for Le Monnier and 0.0077^m for Mare Crisium. The centre of Tycho shows a curved figure with factors of reddening 0.0034^m, 0.0061^m and

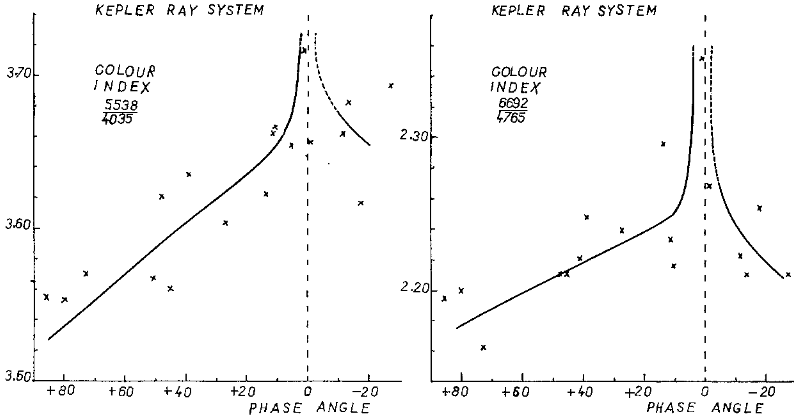

Fig. 20.

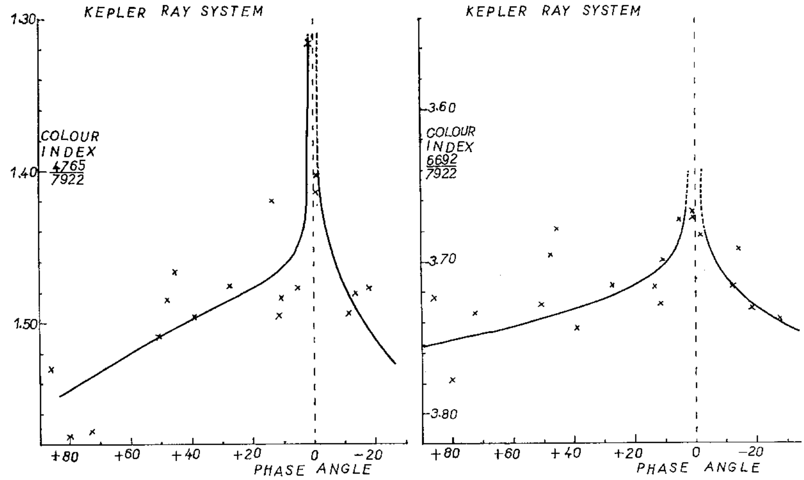

Fig. 21.

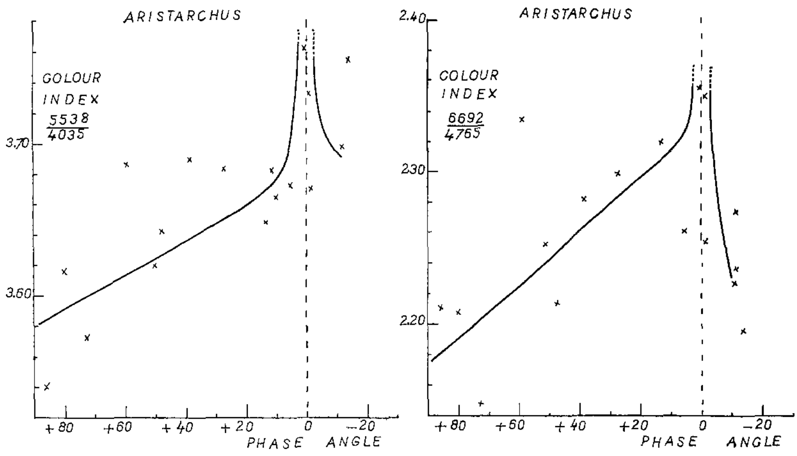

Fig. 22.

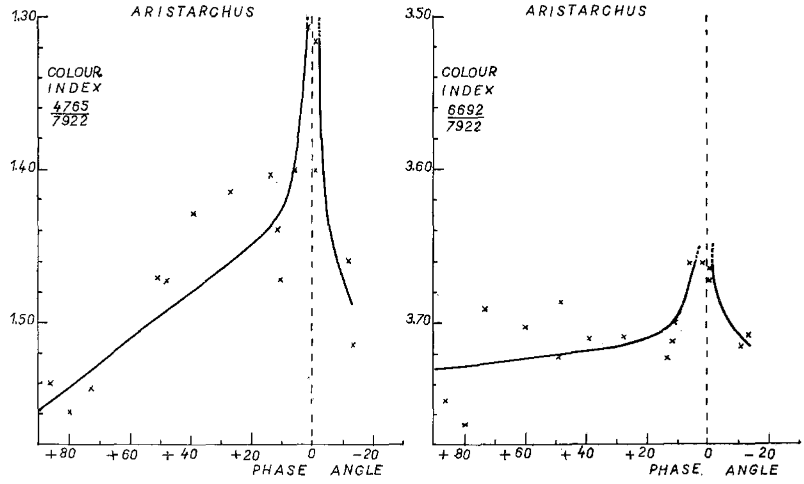

Fig. 23.

0.0019^m per degree corresponding to a range of phase angles ($\alpha = 2°$ and 50°), ($\alpha = 2°$ and 20°) and ($\alpha = 20°$ and 50°) respectively.

Before full Moon, the phase factors of reddening of this colour index are also relatively high and the number of observations and the range of phase angles are small (Table VII).

C. THE COLOUR INDEX $(\frac{4765}{7922})$-PHASE VARIATIONS

The change of the colour of the lunar regions with phase in the case of the colour index $\frac{4765}{7922}$ are shown in Figures 3, 5, and 31. The phase factors of reddening after full Moon, Table VI, show little differences in most of the regions and considerable differences in few regions of the same phase range of observations. The reddening factors are 0.0015^m per degree for Plato, 0.0014^m for Sinus Iridum, 0.0018^m for Archimedes, 0.0013^m for Grimaldi, 0.0008^m for Mare Tranquillitatis, 0.0017^m for Mare Serenitatis, 0.0018^m for Kepler, 0.0013^m for Kepler's Ray System, 0.0016^m for Aristarchus, 0.0018^m for the bright area north-west of Aristarchus and 0.0006^m for Copernicus north. The mean phase factor of reddening for these regions is 0.0014 per degree.

The factors of reddening of Sinus Iridum are 0.0030^m per degree between $\alpha = 5°$ and 40°, 0.0013^m between $\alpha = 40°$ and 86° while it has a mean value of reddening of

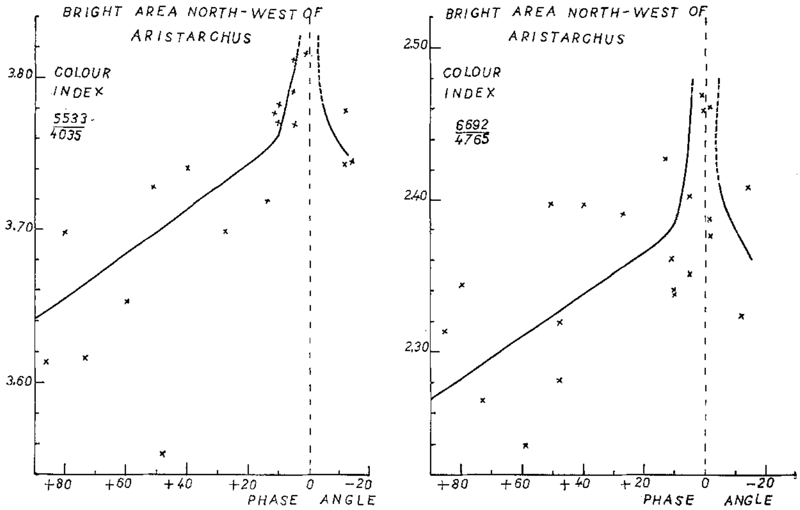

Fig. 24.

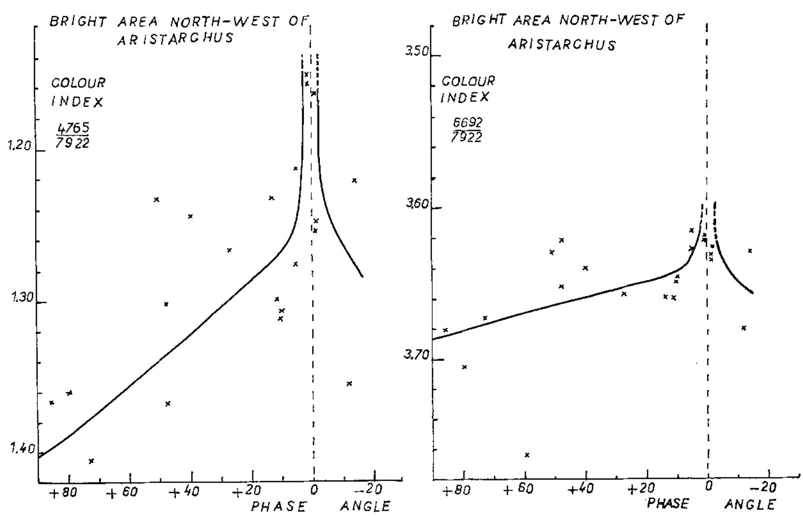

Fig. 25.

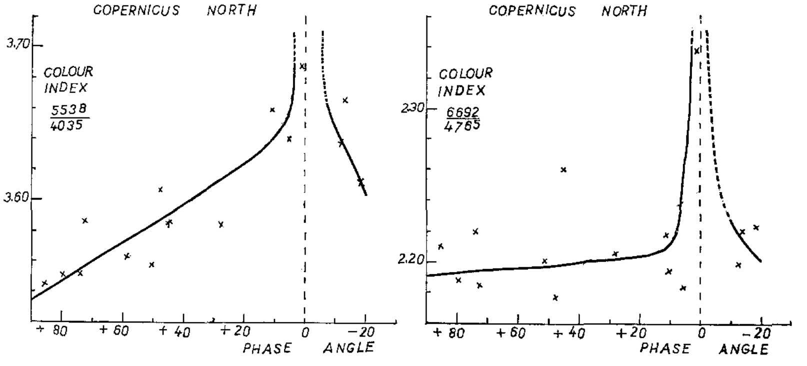

Fig. 26.

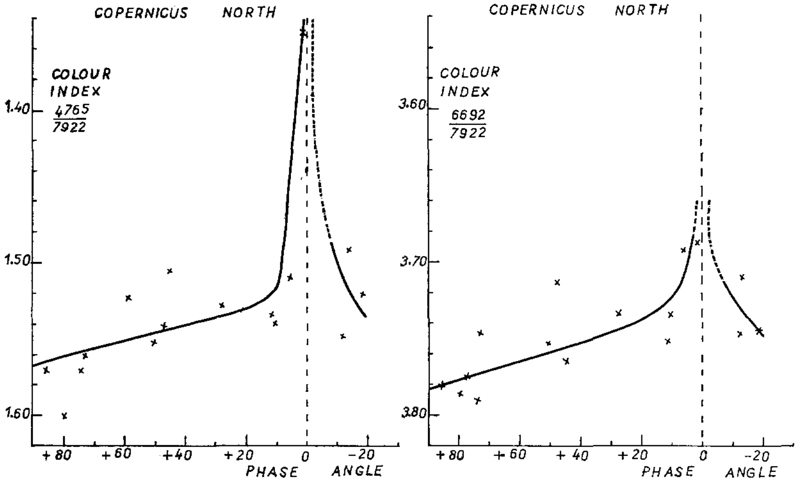

Fig. 27.

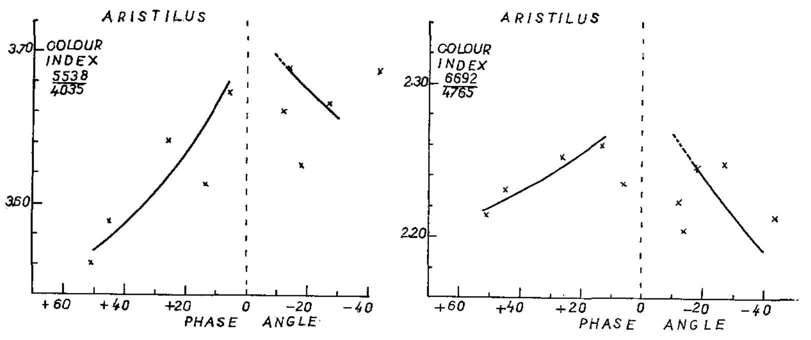

Fig. 28.

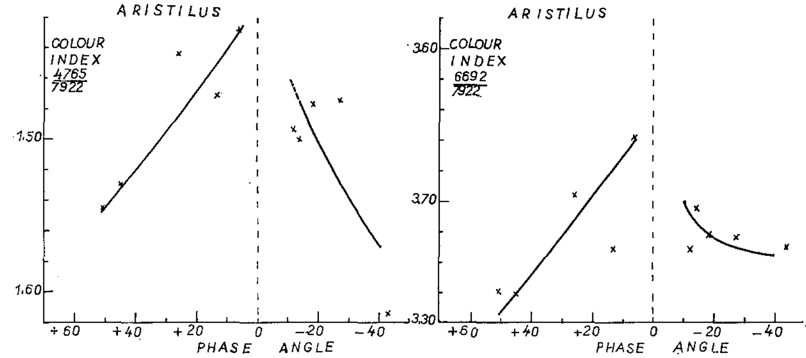

Fig. 29.

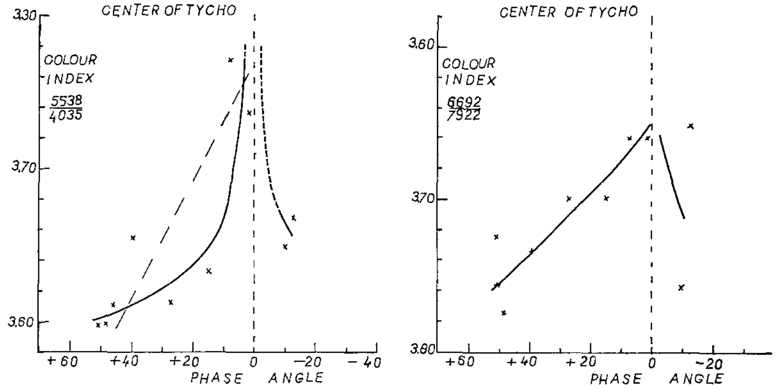

Fig. 30.

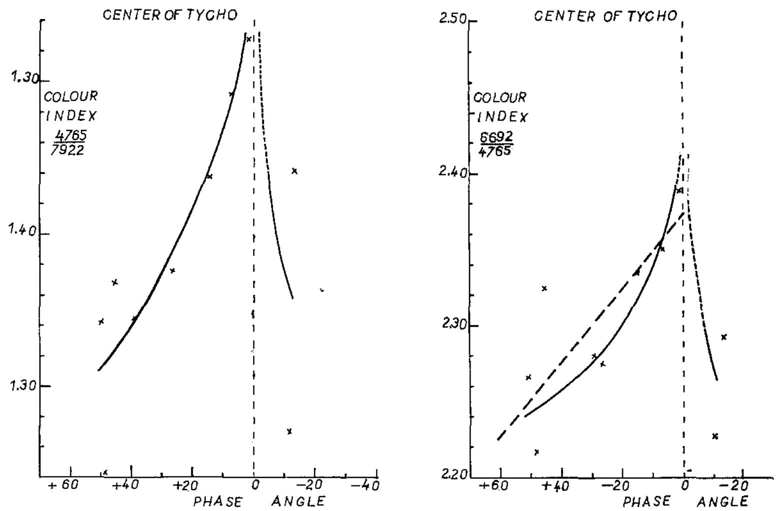

Fig. 31.

0.0014^m per degree between $\alpha=5°$ and $86°$. Centre of Tycho show high reddening phase factors of 0.0062^m per degree between $\alpha=2°$ and $20°$, 0.0036^m between $\alpha=20°$ and $50°$ and of mean factors of 0.0046^m between $\alpha=2°$ and $50°$.

The limited observations in phase angles after full-Moon for Mare Crisium, Le Monnier, Autolycus, Aristillus and centre of Tycho give high reddening factors of 0.0068, 0.0028, 0.0031, 0.0027 and 0.0046^m per degree respectively.

Before full-Moon, the reddening factors are also high in value and the number of observations and the phase angle ranges are small (Table VII).

D. THE COLOUR INDEX $(\frac{6692}{7922})$-PHASE VARIATIONS

After full-Moon, the reddening factors of the colour index at the red end between $\lambda=6692$ Å and $\lambda=7922$ Å are given in Table VI. Excluding Mare Tranquillitatis and one of the areas in Mare Serenitatis, the grounds of photovisual albedo's less than 10% show a similar change of the colour indices with phase, and the reddening factors are 0.0012^m per degree of Plato, 0.0011^m for Sinus Iridum, 0.0013^m for Archimedes, 0.0014^m for Grimaldi, 0.0007^m for Mare Tranquillitatis and 0.0016^m, 0.0010^m and 0.0007^m for the three regions of Mare Serenitatis. Excluding Kepler, the grounds of photovisual albedo's larger than 10% show relatively small reddening factors. These factors are 0.0012^m per degree for Kepler, 0.0007^m for Kepler Ray System, 0.0004^m for Aristarchus, 0.0006^m for the bright area north-west of Aristarchus and 0.0007^m for Copernicus north.

Again, the limited observations in the phase angles, show higher reddening factors which are 0.0025^m for Aristillus, 0.0022^m for the centre of Tycho, 0.0044^m for Mare Crisium, 0.0022^m for Autolycus and 0.0019^m for Le Monnier.

The reddening factors before full-Moon have also higher values than after full-Moon (Table VII).

E. COLOUR-OPPOSITION-EFFECT

The opposition effect which is the non-linear surge in the brightness near full-Moon is established by Gehrels *et al.* (1964). In the present investigation a steep increase in the colour indices near full-Moon is found, for the first time, and is named colour-opposition-effect. This effect is detected because the present observations cover a wide range of phase angles and extend to smaller angles near full-Moon. The smaller scatter in the observations is one of the factors which led to the detection of the phenomena.

As mentioned before, the colour indices are bluest at the time of full-Moon and grow redder towards both quarters. The change of the values of the colour indices arising from the opposition effect are given in Table VIII and are shown in most of the diagrams of Figures 2–31 which are extended to near full-Moon.

The magnitudes of the colour-opposition-effect are different for the grounds investigated on the lunar surface and they are independent of the location of the areas on the disc of the Moon. The effect shows up mostly in the range of 10° on both sides of the full-Moon. There are, however, some grounds in which the effect starts at 5°, 15° and 20° (Table VIII). For the colour index $\left(\frac{4035}{5538}\right)$, the order of reddening in magnitudes near opposition varies from 0.03^m for the area of Le Monnier to 0.12^m for the centre of Tycho. For the colour indices $\left(\frac{4765}{6692}\right)$ and $\left(\frac{4765}{7922}\right)$, the order of reddening in magnitudes of this effect are larger. However, it varies from 0.03^m for Kepler to 0.08^m for Mare Tranquillitatis in the case of the colour index $\left(\frac{6692}{7922}\right)$. As shown in Figures 2–31, the colour index $\left(\frac{6692}{7922}\right)$ show the least colour-opposition-effect.

F. THE REDDENING PHENOMENA

The present investigation shows clearly the reddening phenomena of the lunar grounds. It has been detected in all the colour indices. After full-Moon, between $\alpha = 10°$ and 86° the reddening with phase for the colour index $\left(\frac{4035}{5538}\right)$ shows slight differences between different regions and the mean reddening factor is 0.0015^m per degree. The reddening with phase of the colour index $\left(\frac{4765}{6692}\right)$ is of a mean value of 0.0013^m per degree generally for the grounds of photovisual albedo's larger than 10% and very little reddening generally for the grounds of photovisual albedo's less than 10% in spite of the pronounced reddening at small phases. The reddening with phase detected for the colour index $\frac{4765}{7922}$ show slight differences between different regions and in general, most of the regions give a mean factor of reddening that equals 0.0014^m per degree. The colour index $\frac{6692}{7922}$ shows a mean reddening factor of 0.0007^m per degree generally for the regions of photovisual albedo's larger than 10% and of 0.0011^m per degree generally for the regions of photovisual albedo's less than 10%.

Thus all the colour indices investigated in the present work strongly confirm the reddening of the observed lunar regions which has been detected by Gehrels *et al.* (1964). There is an indication, for the first time, that the reddening factors of certain colour indices are dependent on the reflectivity of the lunar grounds.

Excluding the colour indices $\left(\frac{4765}{6692}\right)$ and $\left(\frac{4765}{7922}\right)$ which cover a wide range of wave-lengths, we can see that the reddening factors are higher in the shorter wave-lengths at the colour index $\left(\frac{4035}{5538}\right)$ than the longer wavelengths at the colour index $\left(\frac{6692}{7922}\right)$ as shown in Tables VI and VII. The values of the reddening factors are independent of the location of the areas on the disc of the Moon.

It has been noticed that higher reddening factors are usually obtained when the observations are taken in a small range of phase angles. This can also be seen in the results of Gehrels *et al.* (1964). This is expected as their reddening factors represent the mean value of reddening at larger and small phase angles.

The results of Wildey and Pohn (1964) showed no clear trend of colour change with phase and the scatter of the points was large. Kenknight *et al.* (1967) restudied the data of Wildey and Pohn and found variation in the colour index (U – V) with phase. They have reported that Wildey and Pohn data do support a reddening with phase amounting to 0.0036 magnitude per degree in the U, V frequency interval which is practically the U, G interval of Gehrels *et al.* (1964). It should be noted here that the reddening factors of Gehrels *et al.* to the average lunar surface are equal to 0.0036 per degree for (U – G). Kenknight *et al.* have concluded from the study of the Wildey and Pohn data, that the reddening with phase seems to be real, but, the deduced factors of reddening 0.0036^m per degree might be uncertain by a factor of two due to the large scatter in the data. In general the phase factors of reddening deduced from the present observations are mostly reduced by a factor of two due to extending the observations to larger phase angles. The observations of Wildey and Pohn (1964) are limited to 28° phase angles and this may be another reason to get high reddening factors. Our data of the present study give high reddening factors when limiting the observations to small phase angle ranges.

The observations of Gehrels *et al.* (1964) have mostly taken between $-45°$ and $+35°$ with observations near full-Moon and when they have extended their range of observations between $-50°$ and $+60°$ they deduced smaller reddening factors. But if they have extended their range of observations beyond this limit, they might be able to detect the kink in the curve near opposition. However, Gehrels *et al.* did point out that the colour phase variations were probably not linear near full-Moon. In general the reddening factors given by Gehrels *et al.* are large because they represent the combined effect of the reddening near full-Moon and that of the wider ranges of phases. Peacock's range of observations (1968) is mainly between $-70<\alpha<+110°$ with a negligible number of observations near full-Moon within $\pm 10°$ of phase angles. This enabled him to obtain small reddening factors. Obviously, the discrepancy between the work of Gehrels *et al.* (1964) and Peacock (1968) concerning the high and the small reddening factors can be explained by the present work. Peacock did not detect colour change with phase in all his pass bands. However, the results of the present work strongly support the reddening phenomena in all the colours investigated agreeing with the results of Gehrels *et al.* (1964).

G. LUMINESCENCE EFFECT

The precision of the colorimetric observations reported in the present work is such that the errors of the individual points plotted in Figures 2–31 are not larger than ± 0.02 magnitude. All the selected grounds are observed with the same equipments and under the same conditions. Therefore, all observations are expected to show the same fluctuation of the colour with phase. This, however, is not found and the dispersion of some points as seen for the figures of some regions is occasionally several times as large. This can in no way be ascribed to observational errors and the possibility of their reality cannot be ruled out. In that case the fluctuation can be explained by the luminescence effect found previously by several workers. The changes are generally observed in the bright regions, especially in the region north-west of Aristarchus, Figures 24 and 25, which show the larger fluctuation of all the observed regions.

6. Possible Interpretations

The present investigation indicates definitely the change of the colour with phase. However, this phenomenon is also detected in some celestial objects like planets and Asteroids. In the case of the planets, the reddening with phase appears clearly in the work of Woolley (1953) and Woolley *et al.* (1955), who have studied the monochromatic magnitudes of Mars' near opposition, while those for Saturn's rings are detected at small phases by Franklin and Cooks (1965). The reddening of the Asteroids has been noticed by Gehrels and Owings (1962).

The colour phase change is generally attributed to scattering by small particles. The explanation of such change on the lunar surface has been approached in two ways. The first way is by the application of Mie's theory while the second is by studying the reddening caused by different samples in the laboratory.

As for the first approach, a model for the lunar surface is given by Gehrels *et al.* (1964) in an attempt to explain the unusual photometric properties of the lunar surface. They considered the Moon to be a sphere covered to a depth of 60 μ by electrostatic suspended particles of 0.8 μ radius and separated by a mean distance of 8 μ. Applying Mie's theory and the calculation performed by Herman and Browning and by Deirmendjian *et al.* (1961) for scattering by particles with small size, Gehrels *et al.* explained the reddening of the lunar surface with phase. The reddening appeared clearly in the previous calculation. However, the Gehrels models is criticized by Hapke (1966) and up till now no sufficient indication of suspended electrostatic particles on the surface of the Moon is given. Further theoretical work concerning multiple scattering may account for the observed reddening as well as for reddening at the opposition.

An approach to detect the reddening with phase has been carried out recently in the laboratory by Coffeen (1965) and Kenknight *et al.* (1967). Coffeen (1965) used the equipment of Gehrels *et al.* (1964) with filters near 0.36, 0.53 and 0.97 μ and deduced the colour of five terrestrial porous samples at phase angles range up to 50°. Three of the samples were porous dust layers of ground volcanic cinder particles smaller than 37 μ in 'fairy-castle' structure. The other two were a porous but solid lava fragment and the fragment covered with a fairy-castle dust layer made from the same lava. The sample was supported such that phases and orientations could be precisely determined. At different phases, the colour indices $(U-G)$ and $(G-I)$ were deduced relative to the colour of sunlight reflected from MgO plates.

In general the factors of reddening of the colour indices of these laboratory samples are not comparable with those deduced for lunar features of the present investigation. Volcanic ash shows high reddening factors. The solid lava fragment is measured only in the colour index $(U-G)$. However, the comparison is not expected as indicated by the soft landings that there is no fairy-castle structure in existence on the lunar surface (Lipsky, 1966). Coffeen's experiment indicates that the reddening factors are different for samples of different properties as well as different change in the colour with phase according to the region of wavelengths used. In addition, an appreciable change in the colour at small phase is detected.

The laboratory studies of Kenknight *et al.* (1957) showed the dependence of the reddening with phase on the colour of the samples. The reddening with phase are confirmed for all the reddish samples while the reddening for gray powders like graphite, SiC, or MgO is vanishing. They suggested that the dependence of colour-phase-effect on the colour of the samples is due to multiple scattering whose extent depends on the albedo and not on the photon frequencies. It is known that the colour index of the lunar surface tends to be correlated to the albedo in the sense that the brighter features are redder (Kopal, 1966). The effect detected by Kenknight *et al.* seems to be similar to that deduced for some lunar regions of the present work for the colour index $(\frac{4765}{6692})$, in the sense that very small reddening factors, are detected for the regions of low albedo at larger phase angles. However, they showed appreciable reddening at small phases. The reddening of the samples at small phases is discussed by Kenknight *et al.* (1967). They reported that the colour of the light back-scattered from a powder changes abruptly at small phase angles if the powder is reddish. But for gray powders there is no colour-phase relationship for large or small phase angles. They suggested that this effect reveals itself at very small phase angles because of the high reflectivity of the dielectric surfaces at glancing incidence and emergence. However, the reddening with phase detected on the lunar surface of the present work show pronounced effect at small phases which is independent of the colour change at larger phases or the reflectivity. But its dependence on the type of the ground (Mikhail, 1968) are explained in the next paragraphs according to the structure of the ground.

Kenknight *et al.* (1967) stated that the opposition effect which is the pronounced increase in the brightness near full-Moon, requires a surface on which there are some pores which are somewhat deeper than they are wide. They added that since the opposition effect is especially marked in forests and grassy fields to an observer in an airplane, the mere occurrence of an opposition effect obviously does not require micron-size particles. Hapke (1963) attributed the opposition effect to the structure of the lunar grounds and in 1965 he discussed the optical properties of the lunar surface and suggested that it may consist of loose clumps of fine particles which themselves are quite complex and are capable of back-scattering strongly, but the porosity instead of being something like 90% which would be the case for the fairy-castle structure, is about 80%. He stated also that the general tendency of the effect of irradiation, to simulate the solar wind hitting the Moon, is to redden rock particles.

The pronounced change in the colour due to opposition effect for the lunar grounds is different than that detected in the laboratory at small phases. The effect detected in laboratory samples is at phases much larger than that detected at lunar surface. This is probably due to the differences in the structures and sizes for particles on the lunar surface and that of the samples. To account for the colour opposition effect detected, in the present work, we surmise that the lunar surface requires loose clumps of fine particles and a certain degree of porosity. The pores are somewhat deeper than they are wide. The upper layers of the lunar surface are exposed to radiation damage which cause the reddening while the lower layers are much less affected. At small phases, the incident sunlight on the lunar surface will penetrate deep into the surface and reflection occurs from all levels. Hence the steep change occurs and the colour becomes bluer representing the optical properties of the lunar surface, at different layers.

The reddening effect of the lunar samples produced by lunar probes may be studied in the laboratory to draw a meaningful analogy with that deduced from all the Earth-based observations.

7. Conclusions

The results obtained in the present investigation covered a wide range of the phase angles and included the region of small phase angles. They confirmed the reddening of the lunar features with increasing phase in the four colour indices studied. It does show clearly the colour opposition effect which could not be detected previously.

The discrepancy between the results of Gehrels *et al.* (1964) and that of Peacock (1968) with respect of the large and small phase factors of reddening can be explained by the present work. There is an indication that the reddening at certain colour indices are dependent on the albedo of the ground. The results as a whole give indication of the luminescence effect found by other workers.

The comparison of the behaviour of the lunar grounds with laboratory samples call for more investigation of Earth samples as well as of lunar samples brought with the astronauts of Apollo 11 and 12.

The results, though interesting in themselves, showed the need for more observations of a large number of selected grounds and of the whole Moon covering a wide range of time and phase. A systematic program would give information of the dependence of the change on the surface brightness and colour. It would be of interest to study the transient colour phenomena of the lunar surface for both short and long period fluctuations and its dependence on solar activity. The present study showed also the need for absolute measurements of the brightness as well as the colour of the selected grounds at different phase angles. However, the program of the present study is wide and will continue for further measurements.

Acknowledgements

The author wishes to express his appreciation to Professor Zdeněk Kopal of the University of Manchester, as well as to Professors Abd El-Hamid Samaha and Adly Salama Asaad of Cairo University for advice and support in this work. He wishes, moreover, to acknowledge the assistance of Dr. K. Peacock, Dr. G. Roberts, and, in particular, of Dr. M. Jones who wrote a computer programme for reductions of the data. Thanks are also due to Mr. F. Abd-el-Badii and Mr. M. Hamdy for help in recording the observations.

References

Coffeen, D. L.: 1965, *Astron. J.* **68**, 49.
Deirmendjian, D., Clasen, R., and Veizee, W.: 1961, *J. Opt. Soc. Am.* **51**, 620.
Franklin, F. A. and Cook, A. F.: 1965, *Astron. J.* **70** **(90)**, 704–720.
Gehrels, T. and Owings, D.: 1962, *Astrophys. J.* **135**, 906.
Gehrels, T., Coffeen, T., and Owings, D.: 1964, *Astron. J.* **69**, 826.
Hapke, B.: 1963, *J. Geophys. Res.* **68**, 4571.
Hapke, B.: 1965, Cornell Research Paper, CRSR, 198.
Hapke, B.: 1966, *Icarus* **5**, 154.

Kenknight, C. E., Rosenberg, D. L., and Wehner, G. K.: 1967, *J. Geophys. Res.* **72**, 3117.
Kopal, Z.: 1962, in *Physics and Astronomy of the Moon* (ed. by Z. Kopal), Academic Press, New York, p. 258.
Kopal, Z.: 1966, *An Introduction to the Study of the Moon*, D. Reidel, Dordrecht, pp. 321–464.
Lipsky, Y. N.: 1966, *Sky Telesc.* **32**, 257.
Mikhail, J. S.: 1968, *Icarus* **8**, 117.
Peacock, K.: 1966, Ph.D. Thesis, University of Manchester.
Peacock, K.: 1968, *Icarus* **9**, 16.
Roberts, G. L.: 1964, M.Sc. Thesis, University of Manchester.
Wildey, R. L. and Pohn, H. A.: 1964, *Astron. J.* **69**, 619.
Woolley, R.v.d.R.: 1953, *Monthly Notices Roy. Astron. Soc.* **113**, 521.
Woolley, R.v.d.R., Gottlieb, K., Heintz, W., and De Vaucouleurs, A.: 1955, *Monthly Notices Roy. Astron. Soc.* **115**, 57.